Anisotropic broadening of the linewidth in the EPR spectra of Cr^{3+} ions in various doped yttrium aluminum garnet single crystals

Xiaoming Bai and Lingwen Zeng
Department of Physics, The Jilin University, Changchun, People's Republic of China
(Received 11 April 1988)

The linewidth in the EPR spectra of Cr^{3+} ions in yttrium aluminum garnet single crystals is investigated at room temperature, and an anisotropic line broadening is observed. The characteristics of broadening resulting from the mosaic effect, internal strains, and fluctuations in the crystalline field parameter CFP are analyzed. A reasonable fit to experimental data is obtained using the hybrid model wherein the mosaic effect, internal strains, and fluctuations in CFP were considered, and the results indicate that the internal strains and fluctuations in CFP are the dominant contributions to linewidth, and the mosaic effect is negligible. The effect of the internal strains caused by impurities in the crystal on linewidth is discussed.

I. INTRODUCTION

The broadening of electron paramagnetic resonance (EPR) spectral lines in single crystals is classified into homogeneous and inhomogeneous broadening. The homogeneous broadening, mainly produced by the dipole-dipole interactions, spin-lattice relaxation, vertical broadening, and fluctuations in microwave frequency, is not important for the anisotropic linewidth of our samples. The mechanisms of inhomogeneous line broadening mainly include the crystal mosaic structure, internal strains produced by defects in the vicinity of the paramagnetic ions, and fluctuations in CFP. Shaltiel *et al.*[1] studied the anisotropic line broadening of EPR spectra of Gd^{3+} ions in ThO_2 caused by the mosaic effect. Feher[2] studied the effect of the uniaxial stresses on the EPR spectra of Mn^{2+} ions in MgO and indicated that a random distribution of internal strains caused by defects in the host would broaden the linewidth. Serway *et al.*[3] investigated the line broadening of EPR spectra of Fe^{3+} in yttrium aluminum garnet (YAG) at 77 K and calculated the linewidth parameters using a hybrid model wherein the mosaic effect, internal strains, and fluctuations in CFP were assumed to be dominant. Their results showed that the major contributions to linewidth arise from the mosaic effect and internal strains. But the angular dependence of linewidth was not given.

Recently Li *et al.*[4] found that with doping Lu^{3+} in YAG:(Nd^{3+},Cr^{3+}) could enhance its laser efficiency. They attributed this effect to the three cations approaching each other as near as possible in order to decrease the elastic potential energy so that the luminescence sensitization from Cr^{3+} to Nd^{3+} would be enhanced. The internal strains caused by inserting Lu^{3+} in YAG:(Nd^{3+},Cr^{3+}) must broaden the EPR spectra of the Cr^3 ion. Therefore the linewidth data of EPR spectra of Cr^{3+} in these three various doped YAG single crystals can provide some information about the mechanism that produces high laser efficiency in YAG:(Nd^{3+},Cr^{3+},Lu^{3+}). In this paper we have studied various mechanisms causing line broadening of EPR spectra of Cr^{3+} in YAG in detail. Misra's[5] least-squares-fitting method was used to fit the experimental data. The effect of impurities in YAG on the linewidth of EPR spectra of Cr^{3+} ions was analyzed qualitatively.

II. EXPERIMENTS

The yttrium aluminum garnet (chemical formula $Y_3Al_5O_{12}$) single crystal has the cubic structure (space group $Ia3d$). The dodecahedral sites are occupied by yttrium ions and the octahedral and tetrahedral sites by aluminum ions. The doped Cr^{3+} ion substitutes for the Al^{3+} ion and enters into the octahedral site. The single crystal samples obtained from the Southwest Technique Physics Institute of China were prepared with high-purity starting materials Y_2O_3 (99.9995% pure) and Al_2O_3 (99.995% pure), and their characteristics were shown in Table I.

The [111] and [110] directions of these three samples were determined by means of the x-ray diffraction method and the errors of the determination were less than 20′ for the [111] axis and 30′ for the [110] axis. The sample whose size is about $3\times3\times1.5$ mm^3 was cemented

TABLE I. The chemical data for samples in experiments.

Sample	Chemical formula	Lattice constant (Å)
YAG:Cr	$Y_{3+0.07}Al_{5-0.004}Cr_{0.004}O_{12}$	12.0081
YAG:(Nd,Cr)	$Y_{3-0.09+0.07}Nd_{0.09}Cr_{0.016}Al_{5-0.016}O_{12}$	12.0097
YAG:(Nd,Lu,Cr)	$Y_{3-0.09+0.035}Nd_{0.09}Lu_{0.035}Cr_{0.016}Al_{5-0.016}O_{12}$	12.0086

on a high-purity quartz pedestal that can rotate around two axes which are perpendicular to each other. The EPR experiment was conducted at room temperature with a Bruker ER-200D-SRC spectrometer operated at the X band. The derivative curve of the EPR absorption was recorded, and the linewidth between the two peaks of the curve was measured in units of gauss with a nuclear magnetic resonance (NMR) gaussmeter. The sample was rotated around the [110] axis and the angle of rotation was measured from one of the [111] axes in the (110) plane to the magnetic-field direction.

III. RESULTS AND ANALYSIS

The linewidths of EPR transitions were recorded when the sample rotated around the [110] axis from 0° to 90° as shown in Fig. 1. The magnetic energy levels relating to these transitions were denoted by 1, 3, 2, and 4 in decreasing sequence. From Fig. 1 we see that there is an anisotropic linewidth in the whole angular variation region for all transitions, an approximate constant and narrow linewidth in some region of angular variation, and a very broad linewidth for the 2-4 transition when angle θ is less than 20°. The linewidth of YAG:(Nd^{3+},Lu^{3+},Cr^{3+}) is the most broad in these different doping samples and that of YAG:Cr^{3+} is the most narrow. The tendency of variation of the angular dependence of linewidth is similar for them. The linewidth for the 3-4 transition when the [111] axis is coincident with the direction of magnetic field is the smallest as the line broadening caused by the mosaic effect, internal strains, and fluctuations in CFP is zero, and is called the residual linewidth which comes mainly from the homogeneous broadening and is assumed to be isotropic. In order to explain the experimental data various mechanisms involving the mosaic effect, internal strains, and fluctuations in CFP are discussed.

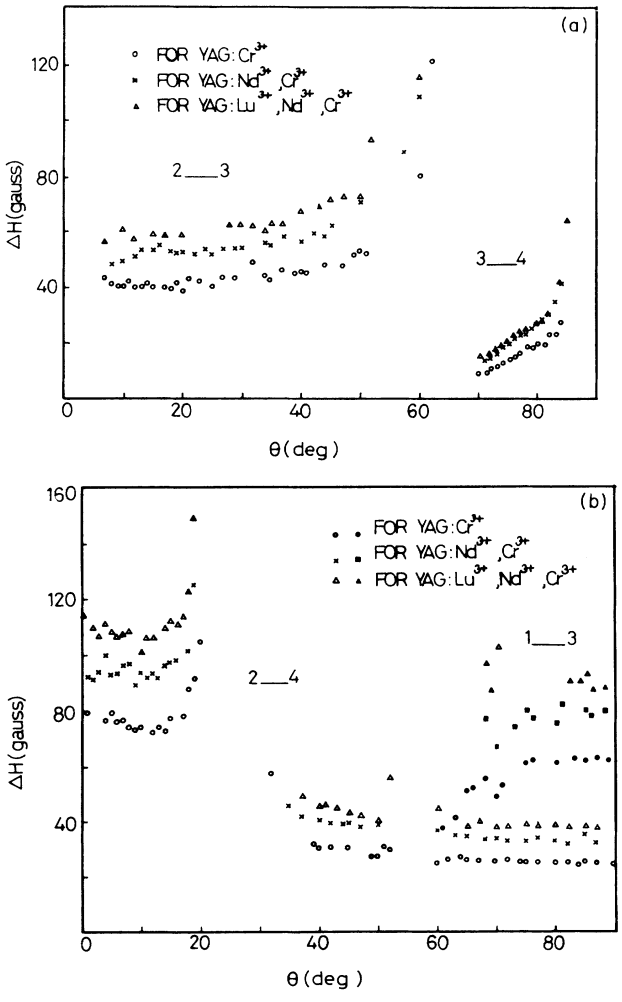

FIG. 1. The experimental angular dependence of the linewidth of Cr^{3+} in various doped YAG, room temperature, X band, (a) for the 2↔3 and 3↔4 transitions, (b) for the 2↔4 and 1↔3 transition.

A. Mosaic effect

The local symmetry axes passing through the sites of Cr^{3+} ions are not exactly parallel among themselves and make a statistical distribution of finite angles about the bulk crystal symmetry axis. In order to simplify the model, an assumption of the distribution being Gaussian type,

$$P(\beta)d\beta=(2/\pi)^{1/2}\Delta\theta^{-1}\exp(-2\beta^2/\Delta\theta^2)d\beta\ , \tag{1}$$

is introduced, where $\Delta\theta$ is the mean width of the local mosaic structure. Now we consider the EPR linewidth of transition between the energy states $|a\rangle$ and $|b\rangle$ which are the linear combination of eigenstates of the Zeeman Hamiltonian of Cr^{3+} ions and are given by:

$$|a\rangle=a_1|\tfrac{3}{2}\rangle+a_2|\tfrac{1}{2}\rangle+a_3|-\tfrac{1}{2}\rangle+a_4|-\tfrac{3}{2}\rangle\ , \tag{2}$$

$$|b\rangle=b_1|\tfrac{3}{2}\rangle+b_2|\tfrac{1}{2}\rangle+b_3|-\tfrac{1}{2}\rangle+b_4|-\tfrac{3}{2}\rangle\ . \tag{3}$$

Then the linewidth contributed from the mosaic effect is

$$\Delta H_m^2=\Delta\theta^2D^2[\sin(2\theta)F/4-\cos(2\theta)G/2 -3\sin(2\theta)E/2]/(\delta\varepsilon/\delta H)\ , \tag{4}$$

where

$$E=2(a_1^2+a_4^2)-2(b_1^2+b_4^2)\ , \tag{5}$$

$$F=(4\sqrt{3})(a_1a_3+a_2a_4-b_1b_3-b_2b_4)\ , \tag{6}$$

$$G=(4\sqrt{3})(a_1a_2-a_3a_4-b_1b_2+b_3b_4)\ , \tag{7}$$

$$\delta\varepsilon/\delta H=(g\beta/2)[3(a_1^2-a_4^2)+(a_2^2-a_3^2) -3(b_1^2-b_4^2)-(b_2^2-b_3^2)]\ . \tag{8}$$

The constants g and D are the spectroscopic splitting factor and zero-field splitting factor, respectively, and are given in Table II. The method for finding g and D was described in detail elsewhere.[6] The angular dependences of linewidth resulting from the mosaic effect for the 2-4 and 2-3 transitions are shown in Fig. 2. The very broad linewidths near 20° for the 2-4 transition and near 60° for the 2-3 transition are conformable to the experimental re-

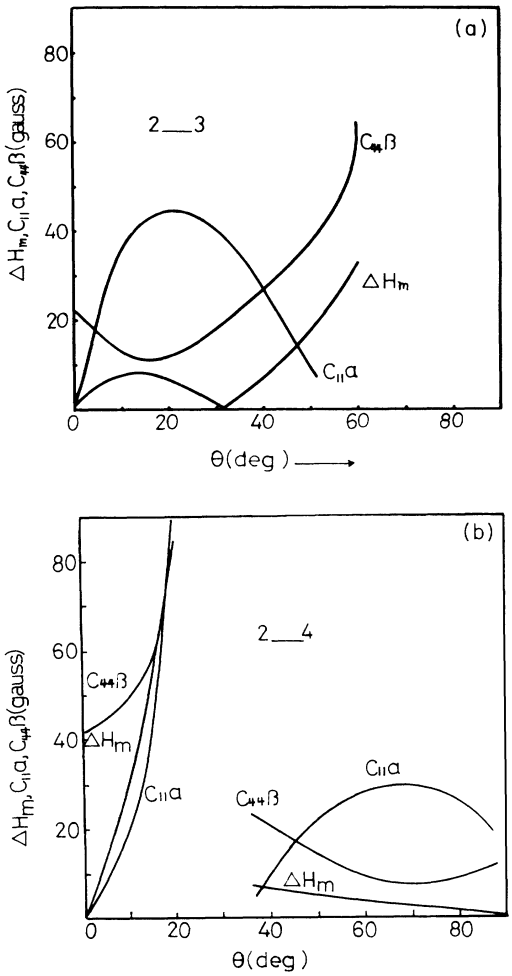

FIG. 2. The theoretical angular dependence curves of the linewidth due to the mosaic effect and parameters $C_{11}\alpha$ and $C_{44}\beta$ in the internal strain model, (a) for the 2↔3 transition, (b) for the 2↔4 transition.

sults, but in other angle regions the theoretical results do not fit to the experimental data at all.

B. Internal strains

The defects in crystal would cause a random distribution of stresses which deviate the atoms or ions from their equilibrium positions. As a result the crystalline electric field at the site of the paramagnetic ion would be distorted. Feher[2] pointed out that the strain-induced perturbation Hamiltonian could be written as $\mathcal{H}_s = \sum_{i,j=1,2,3} S_i D_{ij} S_j$ (1,2,3 denote the cubic axes of the crystal). The tensor D represents the effect of deformation of the system and may be expressed as a linear function of the internal strain, $D_{ij} = \sum_{k,l} C_{ijkl} X_{kl}$, where X_{kl} are the components of the internal strain tensor and C_{ijkl} are called the spin-lattice coefficients, describing the characteristics of the system under considerations. Shulman *et al.*[7] showed that the spin-lattice coefficients would obey similar relations to those obtained between the elastic constants for crystals of cubic symmetry. Namely, in terms of the contracted Voigt notation, $C_{11}=C_{22}=C_{33}$; $C_{44}=C_{55}=C_{66}$; $C_{12}=C_{23}=C_{13}=-C_{11/2}$. We are therefore left with two independent constants, C_{11} and C_{44}. Then the strain-induced perturbation Hamiltonian is given by

$$\begin{aligned}\mathcal{H}_s =& \tfrac{3}{2}C_{11}(X_{11}S_1^2+X_{22}S_2^2+X_{33}S_3^2)\\ &+C_{44}[X_{12}(S_1S_2+S_2S_1)+X_{23}(S_2S_3+S_3S_2)\\ &+X_{31}(S_3S_1+S_1S_3)] .\end{aligned} \tag{9}$$

We assume that the probabilities of the components of the strain tensor are not correlated. As the crystal has the cubic symmetry, the distributions of X_{11}, X_{22}, and X_{33} are equivalent and X_{12}, X_{23}, and X_{13} are equivalent also. These distributions are assumed to be Gaussian type and given by

$$\begin{aligned}P(X_{11}) &= P(X_{22})\\ &= P(X_{33})\\ &= (2/\pi)^{1/2}\alpha^{-1}\exp(-2X_{11}^2/\alpha^2) ,\end{aligned} \tag{10}$$

$$\begin{aligned}P(X_{12}) &= P(X_{23})\\ &= P(X_{13})\\ &= (2/\pi)^{1/2}\beta^{-1}\exp(-2X_{12}^2/\beta^2) .\end{aligned} \tag{11}$$

For convenience we transform the spin operator defined in the crystal coordinate system to the laboratory coordinate system where the z axis is parallel to the direction of magnetic field, and the linewidth resulting from this effect is

$$\begin{aligned}\Delta H_s =& (\tfrac{27}{8}C_{11}^2\alpha^2[F\sin^2\theta'+(1-1.5\sin^2\theta')E-0.5G\sin\theta'\cos\theta']^2\\ &+C_{44}^2\beta^2\{[(1-0.5\sin^2\theta')F+3E\sin^2\theta'+G\sin\theta'\cos\theta']^2\\ &+[0.25F\sin(2\theta)-0.5G\cos(2\theta')-1.5E\sin(2\theta')]^2\})/(\delta\varepsilon/\delta H)^2 ,\end{aligned} \tag{12}$$

TABLE II. The spin-Hamiltonian parameters for samples.

Sample	$g_{\parallel}$	$g_{\perp}$	D (cm^{-1})
YAG:Cr	1.9765±0.0004	1.9765±0.0004	0.2551±0.0002
YAG:(Nd,Cr)	1.9765±0.0004	1.9784±0.0004	0.2550±0.0002
YAG:(Nd,Lu,Cr)	1.9768±0.0004	1.9780±0.0004	0.2555±0.0002

where $\theta' = 54.7° - \theta$ (in deg). The angular dependence of linewidth associated with parameters $C_{11}\alpha$ and $C_{44}\beta$ in Eq. (12) are shown in Fig. 2. It is expected that the appropriate combination of these two parameters would give an approximate constant linewidth in some angular region. Figure 3 represents the linewidth resulting from internal strain when $C_{11}\alpha = 52.3$ MHz and $C_{44}\beta = 56.3$ MHz for YAG:Cr^{3+}.

C. Fluctuations in CFP

The fluctuations in the crystalline electric-field parameter due to some perturbations such as thermal fluctuations would cause broadening of EPR spectral lines of Cr^{3+} ions. If we assume that there is a distribution of CFP about a mean value D and this distribution is Gaussian type, the contribution to the linewidth from this effect is given by

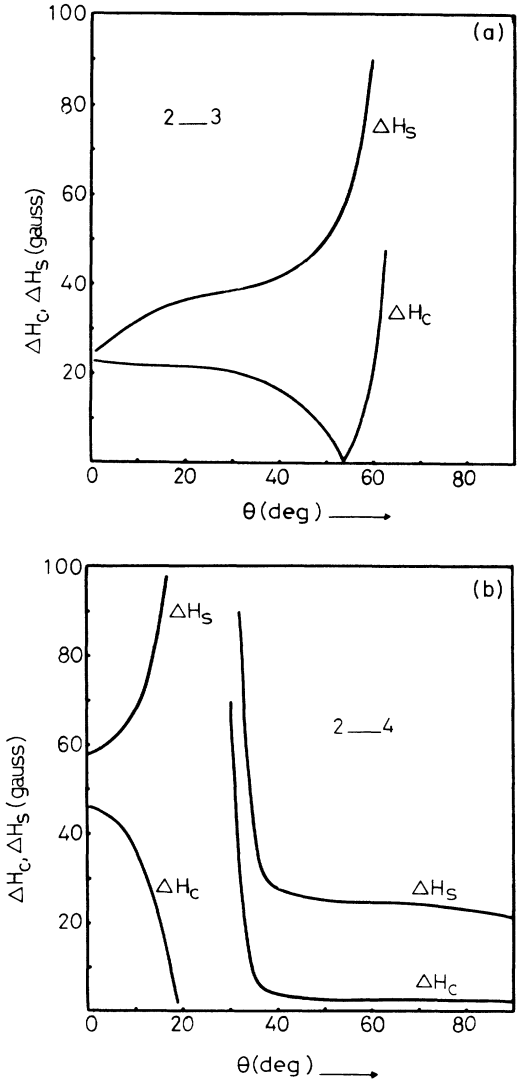

FIG. 3. The theoretical angular dependence curves of the linewidth of Cr^{3+} in YAG:Cr^{3+} when internal strains and fluctuations in CFP were considered, respectively, (a) for the 2↔3 transition, (b) for the 2↔4 transition.

$$\Delta H_c^2 = \Delta C^2[0.25F\sin^2\theta + (1 - 1.5\sin^2\theta)E - 0.5G\sin\theta\cos\theta]^2/(\delta\varepsilon/\delta H)^2 , \quad (13)$$

where ΔC is the mean width of the distribution of CFP.

The linewidth angular dependence from this effect is shown in Fig. 3. It can account for the result of a broad linewidth for the 2-4 transition when θ is less than 20°. Now we see that any one of the three models discussed above cannot explain the experimental data correctly. As all these mechanisms will play some role in line broadening it is necessary to consider them together. In the so-called hybrid model the anisotropic line broadening is assumed to be due to a combination of the internal strains, mosaic effect, and fluctuations in CFP, and the residual linewidth is isotropic and remains the same value for all transitions. If the contributions to the linewidth are statistically independent, the linewidth is given by

$$\Delta H^2 = \Delta H_0^2 + \Delta H_m^2 + \Delta H_s^2 + \Delta H_c^2 , \quad (14)$$

where ΔH_m, ΔH_s, ΔH_c are line broadenings due to the mosaic effect, strains, and fluctuations in CFP which were given in Eqs. (4), (12), and (13), respectively. And ΔH_0 is the residual linewidth whose magnitude equals the value of the linewidth of the 3-4 transition when $\theta = 0°$.

We have used a large amount of experimental data to fit the linewidth parameters (e.g., 79 data were used for YAG:Cr^{3+}). First we calculated the energy eigenvalues and eigenstates corresponding to the resonance field at some angle and the coefficients of the linewidth of various mechanisms using the spin-Hamiltonian parameters in Table II. Then we used the brute force method to fit the linewidth parameters approximately in a wide region of variation of parameters. Finally we used Misra's least-squares-fit (LSF) method to fit the expected linewidth parameters, with the initial values being chosen from those determined by the brute force method. The final results are shown in Table III and the theoretical curves for YAG:Cr^{3+} are shown in Fig. 4. Our results show that the main contributions to the linewidth seem to come

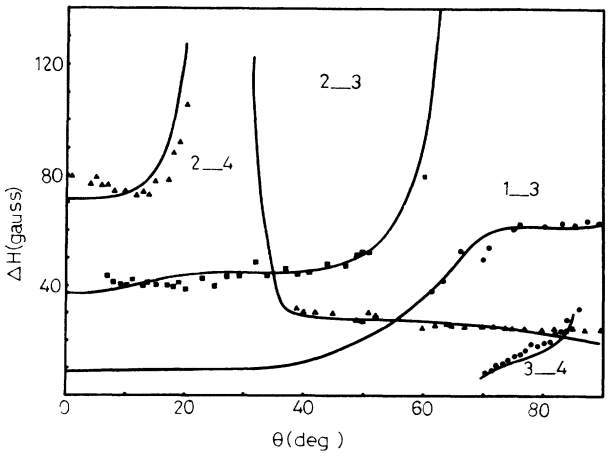

FIG. 4. The theoretical angular dependence curves of Cr^{3+} in YAG:Cr^{3+} when the hybrid model was considered.

TABLE III. The linewidth parameters for the three samples in experiments.

Sample	$\Delta\theta$ (deg)	ΔC (MHz)	$C_{11}\alpha$ (MHz)	$C_{44}\beta$ (MHz)	Uncertainty (%)
YAG:Cr	<0.01	63.4	52.3	56.3	5.3
YAG:(Nd,Cr)	<0.01	56.6	82.7	80.9	7.9
YAG:(Nd,Lu,Cr)	<0.01	61.5	82.7	80.4	7.2

from the internal strains and fluctuations in CFP. The mosaic effect is so small that its effect on line broadening is beyond the determination of our fitting.

IV. DISCUSSIONS

For our samples the contribution to the linewidth from the mosaic effect can be neglected. This result indicates that all local symmetry axes passing through the paramagnetic ions are approximately parallel. This is probably due to the high-purity starting chemicals used in synthesizing and the good quality of crystal. The fluctuations in CFP are caused by some types of perturbation on the paramagnetic ion and its ligand ions. We consider that the thermal motion of ions is an important type of perturbation and it will play a great role at room temperature. This effect enables the linewidth parameter ΔC to become very large. Our results show that the internal strain is a main contribution to the EPR linewidth. As we know, the defects discussed here include all factors which destroy the perfection of the crystal such as impurities, point defects, and so on. It is impossible to study the effect of some one type of defects alone in causing the line broadening. We consider that the impurities in the crystal would be the main source of internal strains, therefore, the linewidth is narrow for YAG:Cr^{3+} because of the low-concentration impurities and broad for YAG:(Nd^{3+},Cr^{3+}) and YAG:(Nd^{3+},Lu^{3+},Cr^{3+}) because of high-concentration impurities. The effect of impurity on the linewidth can be recognized qualitatively from this analysis. The hybrid model gives a more reasonable fit to experimental data and the single model can explain some features. The error in fitting for YAG:Cr^{3+} is small compared with those of the others. This is owing to the different impurity concentrations of those samples. In the case of high impurity concentration the internal strain model must be corrected. Meanwhile the defects in the crystal will correlate to each other so the assumptions of the statistical-independent distribution of components of the strain tensor and the linearity relation between the D tensor and strain tensor are not exact, and the fitting error increases.

The radius of Lu^{3+} ions is less than that of Nd^{3+} ions. Doping Lu^{3+} ions into YAG:(Nd^{3+},Cr^{3+}) would improve the distortions in the lattice caused by doping Nd^{3+} ions in YAG. So the linewidth parameters of the strain model are approximately the same for YAG:(Nd^{3+},Cr^{3+}) and YAG(Nd^{3+},Cr^{3+},Lu^{3+}).

Our theoretical results indicate that the contribution to line broadening from the internal strain effect has some parts in angular dependence similar to those from the mosaic effect. If we use the single mosaic model to analyze the linewidth angular dependence as Serway did, the effect parameter of the linewidth determined is

$$\Delta\theta_s^2=\Delta\theta_m^2+[(\cos 110^\circ)C_{44}\beta/D]^2 , \tag{15}$$

where $\Delta\theta_m$ corresponds to the mean mosaic angle and $\Delta\theta_s$ corresponds to that determined by Serway. This point was neglected in Serway's work. For YAG:Cr^{3+} this correction is

$$\Delta\theta_{\text{correct}}=(\cos 110^\circ)C_{44}\beta/d+0.14^\circ . \tag{16}$$

So we say that the neglect of this correction is not reasonable when the internal strains in the crystal are large. The discrepancies between the observed and calculated results of the 2-4 transition in the 0°–20° angle region might be the result of neglecting the higher correction terms in calculating ΔH_s and ΔH_m, which must be considered because the slope of the isofrequency curve is much larger in this angular region.

ACKNOWLEDGMENTS

We would like to express our appreciation to Professor Daiming Wu for some meaningful discussions, Professor Qingyong Zhai and Dr. Qikang Li for the supplying of samples, and Lixin Wu for help in using the computer.

[1]D. Shaltiel and W. Low, Phys. Rev. **124**, 1062 (1961).
[2]E. Rosenvasser Feher, Phys. Rev. **136**, A145 (1964).
[3]R. A. Serway, F. H. Yang, and S. A. Marshall, Phys. Status Solidi B **89**, 267 (1978).
[4]Q. K. Li and Q. Y. Zhai (unpublished).
[5]S. K. Misra, J. Magn. Reson. **23**, 403 (1976).
[6]Y. Li and L. W. Zeng, in *Proceedings of the 2nd Beijing Conference and Exhibition on Instrumental Analysis, Beijing, China, 1987* (BCEIA, Beijing, 1987), p. 1165.
[7]R. G. Shulman, B. S. Wyluda, and P. W. Anderson, Phys. Rev. **107**, 953 (1957).